Responses of *Mytilus galloprovincialis* to challenge with environmental isolates of the potential emerging pathogen *Malaciobacter marinus*

Manon Auguste[1*], Faiz Ur Rahman[2,3], Teresa Balbi[1], Martina Leonessi[1], Caterina Oliveri[1], Grazia Bellese[4], Luigi Vezzulli[1], Dolors Furones[2], Laura Canesi[1]

[1]DISTAV, Dept. of Environmental, Earth and Life Sciences, University of Genoa, Italy
[2]IRTA_Sant Carles de la Ràpita Centre, Aquaculture Program, Spain
[3]Unit of Microbiology, Department of Basic Health Sciences, Faculty of Medicine and Health Sciences, IISPV, Universitat Rovira i Virgili, Reus, Spain.
[4] DIMES, Dept. of Experimental Medicine, University of Genoa, Italy
**Corresponding author*

Abstract

Bacteria of the *Arcobacter*-like spp. represent emerging foodborne zoonotic pathogens in humans and animals. Their increasing presence in seafood, suggesting higher occurrence in seawater due to marine pollution, is raising some environmental concern. Although *Arcobacter* is frequently detected in diseased oysters and stressed bivalve species, no data are available so far on its potential pathogenicity or interactions with the immune system of the bivalve host.
In this work, responses to challenge with two strains of *Malaciobacter marinus* IRTA-19-131 and IRTA-19-132, R1 and R2), isolated from adult *Crassostrea gigas* during a mortality event in 2019 in Spain, were investigated in the mussel *Mytilus galloprovincialis*.
In vivo experiments were performed in larvae (48 h post-fertilization), and in adult mussels at 24 h post-injection, in order to evaluate the pathogenicity for early developmental stages, and the hemolymph immune responses, respectively. Both R1 and R2 were moderately pathogenic to early larvae, with significant decreases in the development of normal D-veligers from 10^4 and 10^3 CFU/mL, respectively. In adults, both strains decreased hemocyte lysosomal membrane stability (LMS), and stimulated extracellular defense responses (ROS production and lysozyme activity).
The interactions between mussel hemocytes and *M. marinus* were investigated in *in vitro* short-term experiments (30-90 min) using the R1 strain (10^6-10^8 CFU/mL). R1 decreased LMS and induced lysosomal enlargement, but not cell detachment or death, and stimulated extracellular ROS production and lysozyme release, confirming *in vivo* data. Moreover, lysosomal internalization and degradation of bacteria were observed, together with changes in levels of activated mTor and LC3, indicating phagocytic activity. Overall, the results indicate the activation of both extracellular and intracellular immune defenses against *M. marinus* R1. Accordingly, these responses resulted in a significant hemolymph bactericidal activity, with a large contribution of hemolymph serum.
The results represent the first data on the potential pathogenicity of *Arcobacter* isolated from a shellfish mortality to bivalve larvae and adults, and on their interactions with the immune system of the host.

Keywords: bivalves, *Malaciobacter marinus*, mussel, larvae, hemocytes, immune response, mTor, LC3

1. Introduction

In the last decades, aquacultured bivalves have been increasingly subjected to recurrent disease outbreaks resulting in mass mortality events. Although juveniles of the Pacific oyster (*Crassostrea gigas*) are the most severely affected, the occurrence of heterogeneous mortalities has been described in adults and other species such as mussels [1–3]. The causes of the disease processes that lead to mass mortality are not always evident; however, it is commonly accepted that these episodes are polymicrobial and multifactorial, involving both host and environmental factors (e.g. bivalves species, genetics and age, temperature, food availability, microbiota, pollutant exposure) [3]. Whatever the source and degree of infection, the outcome of the response to potential pathogens depends on complex interactions between the immune system of the host and the associated microbial communities [4]. Recent studies have reported the recurrent presence of bacteria of the genus *Arcobacte*r in oysters (*C. gigas*) during mortality episodes [5,6]. Similar observations were made in laboratory experiments in oysters immune-compromised by OsHV-1 [7] or oysters and mussels exposed to temperature stress [8,9]. In mussels (*Mytilus galloprovincialis*) exposed to nanoplastics, an increased abundance of *Arcobacter* in hemolymph microbiome was observed [10].

Arcobacter spp. are recently regarded as emerging foodborne pathogens affecting both humans and animals, with the most common *A. butzleri* (reviewed in [11]). *Arcobacter* have been shown to inhabit very diverse environments, including sewage water [12]. Even though some *Arcobacter* species are believed to be free-living, waterborne organisms, and autochthonous to aquatic environments, they are also naturally present in bivalve microbiome [13,14]. While some species were found only in mussels (e.g. *A. mytili*) [15], the presence of others seems to be due to fecally contaminated freshwater inputs, as the presence of *A. butzleri* was correlated with the levels of *Escherichia coli* [16]. Since bivalves represent a cause of foodborne disease in humans, available literature mainly focuses on the detection of *Arcobacter* in edible species [11,14,16–18]. However, no data are available yet on the capacity of bivalves to respond to infection with *Arcobacter* and on the interactions with their immune system. Therefore, it is not clear if *Arcobacter* members can represent primary or opportunistic pathogens for different bivalves.

In this work, responses to challenge with two strains of *Malaciobacter marinus* isolated from *C. gigas* during a mortality event in 2019 in the Ebro delta in Spain (IRTA-19-131 and IRTA-19-132) were investigated in the Mediterranean mussel *M. galloprovincialis*. *In vivo* experiments were performed in larvae (48 h post-fertilization, hpf), and in adult mussels at 24 h post-injection (p.i.), in order to evaluate the pathogenicity for early developmental stages, and the hemolymph immune responses, respectively. The interactions with mussel hemolymph components and the mechanisms involved in the immune response were investigated in *in vitro* short-term experiments with IRTA-19-131. This work is part of a wider study on the epidemiology of *M. marinus* in the Ebro delta, along with the screening of other bacterial and viral pathogens, and on the *in vivo* pathogenicity of *M. marinus* in oysters.

2. Methods

2.1 Bacterial isolation and identification

Bacterial strains (IRTA-19-131 and IRTA-19-132) for challenge experiments were isolated from adult diseased oysters (*C. gigas*) collected during a mortality event that occurred in Fangar bay (40° 46.506'N; 0° 44.246'E, Ebro Delta, Spain) in June 2019. Briefly, aliquots (1 mL) of whole oyster tissue homogenates (from a pool of 5 oysters) were added with 9 mL of *Arcobacter* broth (Sigma-Aldrich, CM0965, Steinheim, Germany) supplemented with CAT [(C.A.T

selective supplement: Cefoperazone-Amphotericin B-Teicoplanin) OxoidTM, SR0174E, Hampshire, UK] and 50% artificial seawater [19] and incubated aerobically at 23 ºC in static conditions. After 48 h the tubes were vortexed for 10 sec and aliquots of 100 µL were transferred to Marine Agar (MA) (Scharlab, 109352, Sentmenat, Spain) plates overlaid with 0.45 µm nitrocellulose membrane filters of (Millipore, Ref # HAWP04700, Tullagreen, Ireland) to retain larger bacteria. After 30 min, the filters were removed, and the plates were incubated aerobically at 23 ºC for 48 h. *Arcobacter*-like spp. (i.e., small, transparent/translucent, beige, or off-white colonies) were sub-cultured on MA medium and incubated in the conditions mentioned above. Genomic DNA (gDNA) was extracted from bacterial isolates using QIAGEN DNeasy® Blood & Tissue Kit (QIAGEN, Ref # 69506, Hilden, Germany). Identification of the isolates was conducted by *Arcobacter* 23S genus specific qPCR and amplification and sequencing of the *rpoB* phylogenetic marker gene as previously described (GenBank accession numbers *rpoB*: OP441048 and OP441049) [15, 20, 21]. Two bacterial isolates were identified as belonging to the species *M. marinus* (IRTA-19-131 and IRTA-19-132).

2.2 Bacterial cultures and inoculum preparation

IRTA-19-131 and IRTA-19-132 strains (henceforth indicated as R1 and R2, respectively) were cultured in *Arcobacter* broth (conventional broth media containing peptone 18 g/L, yeast extract 1g/L, NaCl 5g/L modified with the addition of 50% artificial seawater-ASW) at 30 °C in a water bath with continuous agitation. After 24 h growth, the inoculum was centrifuged (4500 × *g*, 20 min), and the pellet was resuspended to obtain a concentration of about 10^8 colony forming units CFU/mL (determined spectrophotometrically as an Abs_{600}=0.20). MA was used throughout the experiments.

2.3. Effects of M. marinus R1 and R2 strains on mussel early larval development

Sexually mature mussels (*M. galloprovincialis*), 4–5 cm long, purchased in February 2021 from an aquaculture farm (La Spezia, Liguria, Italy) were acclimated in tanks with aerated artificial seawater (ASW), salinity 35 ppt (1 L/mussel) at 18 °C and utilized within 2 days for gamete collection [22]. The 48 h embryotoxicity assay was carried out in 96-microwell plates as in Balbi et al. (2019) [23]. At 30 min post-fertilization, aliquots of R1 and R2, from a 10^8 CFU/mL stock suspension, were tenfold serially diluted in ASW and added to fertilized eggs in each microwell to reach the desired nominal final concentrations (from 10^2 to 10^7 CFU/mL) in a 200 µL volume. Microplates were then incubated for 48 h at 18 °C ± 1 °C, with a 16:8 h light: dark photoperiod. All the procedures were carried out following ASTM [24]. At the end of incubation, each sample was fixed with buffered formalin (4%) and all larvae examined by optical microscopy using an inverted Olympus IX53 microscope (Olympus, Milano, Italy) at 40 ×, equipped with a CCD UC30 camera and a digital image acquisition software (cellSens Entry). A D-shaped (straight hinge) larva with no protruding mantle was considered normal; if the typical stage at 48 hpf was not reached (trochophore or earlier stages) or when some developmental impairments were observed (concave, malformed or damaged shell, protruding mantle), the larva was considered malformed. The acceptability of test results was based on controls for a percentage of normal D-shell larvae >75% [24].

2.4 In vivo challenge of adult mussels with M. marinus R1 and R2 strains

Adult mussels (*M. galloprovincialis*), 4–5 cm long, were purchased in summer 2021 and acclimated in tanks with aerated artificial seawater (ASW) for 24 h, salinity 35 ppt (1 L/mussel) at 18 °C. Animals (20 mussels per condition) were injected into the posterior adductor muscle as previously described [23] utilizing 50 µL of live bacterial suspensions (*M. marinus* R1 or R2) containing 10^8 CFU/mL in PBS+NaCl (phosphate-buffered solution isotonic with

hemolymph, PBS+NaCl: 2 mM KH_2HPO_4, 10 mM Na_2HPO_4, 3 mM KCl, 600 mM NaCl in distilled water, pH 7.4), in order to obtain a nominal concentration of 5×10^6 CFU/mL hemolymph. Control mussels were injected with PBS+NaCl. No mortality was observed during the experiments. At 24 h post-injection (p.i.), hemolymph was collected from the posterior adductor muscle of 4 pools of 4 mussels each. Hemocyte LMS, reactive oxygen species (ROS) production, and soluble lysozyme activity were determined in whole hemolymph samples from control and exposed groups. Hemolymph collection and assays were performed as previously described [23,25,26].

2.5 In vitro challenge of Mytilus hemocytes with M. marinus R1 strain

2.5.1 Hemolymph sampling and monolayer preparation

Using a sterile 1 mL syringe with an 18 G1/2″ needle, the hemolymph was extracted from the posterior adductor muscle. The hemolymph, with the needle prior removed, was filtered through sterile gauze and pooled at 18 °C. For hemocyte monolayers preparation, 20 µL drops of the whole hemolymph were deposited on microscope slides and the cells were let to adhere for 20 min before removing the excess of hemolymph. To obtain hemolymph serum-HS, the whole hemolymph was centrifuged at 100 × *g* for 10 min, and the supernatant was sterilized through a 0.22 µm-pore filter. Hemocyte monolayers or whole hemolymph (according to the endpoint, see details in the next sections) were incubated with *M. marinus* R1 suspension suitably diluted in ASW or HS at different concentrations (10^6, 10^7, 10^8 CFU/mL) from 30 to 90 min, depending on the endpoint measured. Untreated samples in ASW or HS were run in parallel. Filter-sterilized ASW was utilized in all experiments.

2.5.2 Determination of functional parameters

All assays were carried out as previously described [23,25,26]. Lysosomal membrane stability (LMS) was evaluated in hemocytes monolayers by the Neutral Red Retention Time (NRRT). Hemocyte monolayers were pre-incubated for 30 min with different concentrations (10^6, 10^7, 10^8 CFU/mL) of *M. marinus* in ASW or HS. Samples were washed out and incubated with a neutral red (NR) (Sigma-Aldrich, Milan, Italy) solution (40 µg/mL in ASW). After 15 min, after removal of excess dye, a drop of ASW was added, and slides were observed under an optical microscope from time zero every 15 min, and the percentage of cells showing loss of dye from lysosomes in each field (10 fields each containing 8-10 cells) was evaluated until 50% of the cells showed sign of lysosomal leaking, i.e., the cytosol becoming red, and the cells rounded. All incubations were carried out at 18 °C.

For the determination of Lysozyme release and ROS production, aliquots of 400 µl of whole hemolymph were incubated with suspensions of *M. marinus* in ASW or HS (final concentrations 10^6 and 10^7 CFU/mL) for different times. Lysozyme activity in the extracellular medium after incubation with bacteria for 0, 30 and 60 min. was evaluated spectrophotometrically at 450 nm using a suspension of *Micrococcus lysodeikticus* (15 mg/100 mL in 66 mM phosphate buffer, pH 6.4). Hen egg white (HEW) lysozyme was used as a standard and lysozyme activity was expressed as HEW lysozyme equivalents (U/mg protein/mL). Extracellular ROS generation was measured by the reduction of cytochrome *c*. Hemolymph samples were incubated for 30 min with a cytochrome *c* solution (75 µM ferricytochrome *c* in TBS (0.05M Tris-HCl buffer, pH 7.6, containing 2% NaCl)). Cytochrome *c* in TBS was used as a blank. Samples were read at 550 nm against cytochrome *c* in TBS as a blank and the results were expressed as changes in OD per mg protein. All data are reported as

percentage of control values. Protein content was determined using the Bradford method with bovine serum albumin (BSA) as a standard.
For *in vivo* experiments, functional parameters were evaluated directly on hemolymph samples after challenge with R1 or R2.

2.5.3 Giemsa Staining

Hemocyte monolayers on microscope slides were incubated for 30 and 90 min with *M. marinus* R1. Samples were washed out, fixed in >50% methanol, and stained with a Giemsa kit (Diff-QuikTM, Medion Grifols Diagnostics AG, Switzerland), following the manufacturer instructions.

2.5.4. Electrophoresis and Western blotting

Hemocyte monolayers were incubated with bacterial suspensions in ASW (10^7 CFU/mL) at 18 °C for 30 and 90 min. Control samples were run in parallel. All procedures were carried out as previously described [26]. Supernatants from each culture dish were discarded and the hemocytes were lysed with 0.1 vol of ice-cold lysis buffer (50 mM Tris-HCl pH 7.8, 0.25 M sucrose, 1% SDS, 2 mM sodium orthovanadate, 0.1% Nonidet-P40, 5 mM M DTT) with protease inhibitors cocktail and phosphatase inhibitors cocktail (Roche, Basel, Switzerland). Samples were boiled for 4 min. and then centrifuged for 20 min. at 14,000 × *g* to remove insoluble debris. Levels of target proteins were determined by SDS-PAGE and Western blotting using specific antibodies as previously described [26]. Samples were probed with rabbit polyclonal anti-LC3 (Sigma-Aldrich, L8918) antibodies (1:500), rabbit polyclonal mTor (phospho S2481) (www.abcam.com, ab137133) (1:1000) and rabbit polyclonal anti-actin antibody (Sigma-Aldrich, A5060) (1:500) as primary antibodies, and with horseradish peroxidase-conjugated goat anti-rabbit IgG (Invitrogen G21234) (1:3000) as secondary antibodies. Immune complexes were visualized using an enhanced chemiluminescence Western blotting analysis system (PURECL-Chemiluminescence Substrate Vilber) following the manufacturer's specifications. Western blotting films were digitized (Chemidoc-Biorad) and band optical densities (arbitrary units) were quantified using a computerized imaging system (QuantityOne).

2.5.5. Bactericidal activity

In vitro bactericidal activity of hemocyte monolayers was evaluated as previously described [23,25]. Hemocytes were incubated with *M. marinus* R1 (5×10^6 CFU/mL) at 18 °C in ASW or HS for different periods of time (0, 30 and 90 min). The bactericidal activity of HS was also evaluated. *M. marinus* in ASW was used as a control for bacterial growth over the experimental time. Immediately after the inoculum (T = 0) and after 30 and 90 min of incubation, supernatants were collected and hemocytes were lysed by adding filter-sterilized ASW supplemented with 0.05% Triton x-100 and by 10 sec agitation. Supernatants and lysates were pooled and tenfold serial diluted in ASW. Aliquots (100 µL) of the diluted samples were plated onto MA. Samples of *M. marinus* suspensions in ASW or HS at the same concentrations were directly diluted and plated. After 48 h incubation at 30 °C, the number of CFU per hemocyte monolayer (representing live, culturable bacteria) was determined. Percentages of killing were determined in comparison to values obtained at zero time. The number of CFU in control hemocytes never exceeded 0.1% of those enumerated in experimental samples.

2.6. Data analysis

Data from *in vitro* and *in vivo* experiments on hemocyte and hemolymph functional parameters are the mean ± SD of at least 4 independent experiments, with each assay performed in triplicate. Statistical analyses were performed by the non-parametric Kruskal-Wallis test followed by Dunn's test ($p \leq 0.05$). Embryotoxicity test data, representing the mean ± SD of 4 independent experiments, carried out in 6 replicate samples in 96-microwell plates, were analyzed by ANOVA plus Tukey's post-test. Data from WB were analyzed by non parametric Mann-Whitney U test. All statistical calculations were performed using the GraphPad Prism version 7.03 for Windows, GraphPad Software, San Diego, CA, USA.

3. Results

3.1 Effects of M. marinus strains R1 and R2 on mussel early larval development

Fertilized eggs were exposed to either R1 or R2 in a wide concentration range (from 10^2 to 10^7 CFU/mL) and the percentage of normal D-larvae at 48 hpf was evaluated as previously described [5,23]. The results are reported in Fig. 1. Exposure to both strains moderately affected normal development, with significant effects for R1 from 10^4 CFU/mL and for R2 from 10^3 CFU/mL. At the maximal concentration tested, the effect of R1 was slightly stronger than that of R2 (with a -38% and -25% decrease in normal larvae, respectively). Interestingly, as shown by representative images, R1 mainly induced a delayed larval phenotype (immature veligers with protruding mantle and incomplete shell formation), whereas exposure to R2 mainly resulted in shell malformations (convex shell hinge).

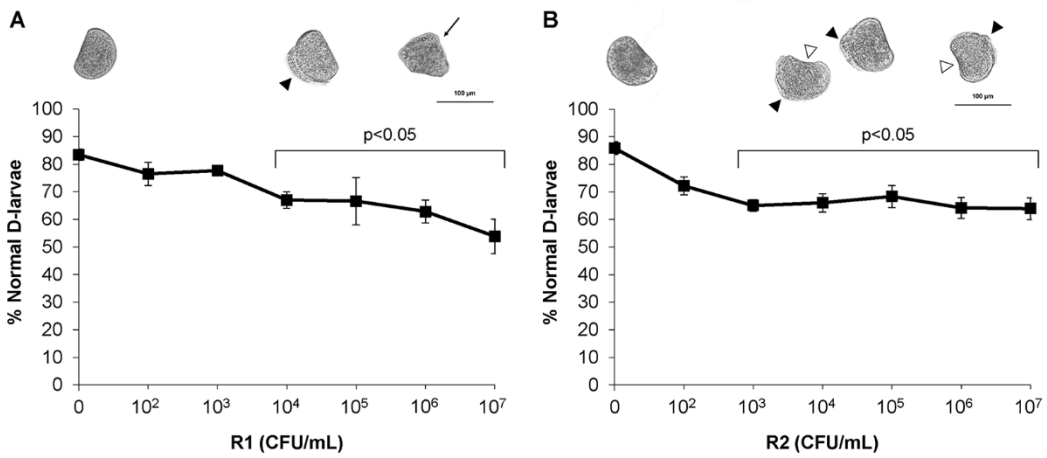

Figure 1. Effects of different concentrations of *M. marinus* strains R1 and R2 on *M. galloprovincialis* larval development at 48 hpf. Percentage of normal D-shaped larvae with respect to controls after exposure to R1 (A) and R2 (B). Data, representing the mean ± SD of 4 experiments carried out in 96-multiwell plates, were analyzed by ANOVA plus Tukey's post-test ($p < 0.05$). Representative images of control larvae and of the main larval phenotypes (lateral view) observed in different experimental conditions at 48 hpf are reported (scale bar: 100 μm). Black arrowhead = protruding mantle; arrow = immature larva (pre-veligers); white arrowhead = convex hinge.

3.2 Effects of in vivo challenge of adult mussels with two M. marinus strains R1 and R2

The effects of *in vivo* challenge of mussels with *M. marinus* R1 and R2 were compared. Bacteria were injected into the posterior adductor muscle to reach a final nominal concentration

of 5×10^6 CFU/mL in hemolymph. After 24 h p.i. the hemolymph was collected and functional immune parameters were evaluated (Fig. 2). Similar responses were observed with both strains. A significant decrease in LMS, evaluated as a marker of cellular stress, was observed (about -60 and -73% with respect to controls for R1 and R2, respectively) (Fig. 2A). This effect was accompanied by a large stimulation of extracellular ROS production (about +400% with respect to controls) (Fig. 2B) and of soluble lysozyme activity (+280% with respect to controls) (Fig. 2C) for both R1 and R2.

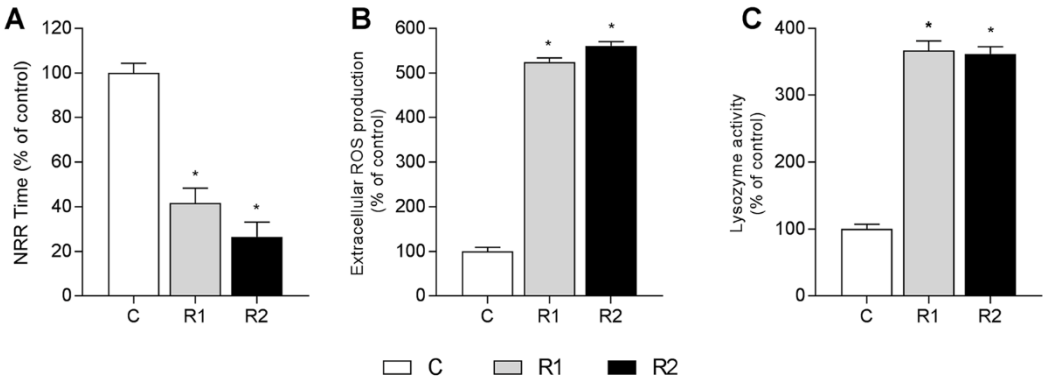

Figure 2. ***In vivo* effects of two *M. marinus* strains R1 and R2 on hemolymph parameters of *M. galloprovincialis*.** Hemocyte lysosomal membrane stability-LMS (A), ROS production (B) and serum lysozyme activity (C) were evaluated in hemolymph sampled from mussels challenged with either R1 or R2 at 24 h p.i. Data are the mean ± SD of 4 independent experiments performed in triplicate. Statistical analyses were performed by non-parametric Kruskal–Wallis followed by Dunn's multiple comparisons test ($p < 0.05$).

3.3 Effects of in vitro challenge of Mytilus hemocytes with M. marinus R1

The effects of *in vitro* short-term incubation (30 min) with different concentrations of the *M. marinus* strain R1 on hemocyte LMS were compared utilizing bacterial suspensions in different media, ASW or HS, and the results are reported in Fig. 3. A dose-dependent decrease in LMS was recorded in both media (Fig. 3A). Significant effects were observed from the lowest concentration tested (10^6 CFU/mL), with a -45% decrease in LMS with respect to control, until almost complete destabilization (> 95%) at the highest concentration tested (10^8 CFU/mL). The effects of R1 on hemocyte LMS were compared with those of the R2 strain in similar experimental conditions. Since similar dose-dependent effects were observed (Fig. S1), subsequent *in vitro* experiments were carried out only with R1.

Early lysosomal changes induced by R1 in live hemocytes could be appreciated from the beginning of the NRR assay (see representative images in Fig. 3B obtained at time 0, after incubation with bacteria, washing and NR loading). In control samples (C), healthy hemocytes were characterized by the presence of numerous small NR loaded vesicles, representing individual lysosomes. In samples challenged with R1, lysosomal enlargement and fusion were observed at increasing concentrations of bacteria. Interestingly, at the end of the assay, when lysosomal destabilization was observed in > 50% of hemocytes (corresponding to data shown in Fig. 3A), the cells remained fully adherent to the substrate, with no appreciable cell detachment and rounding typical of dying cells (Fig.S2).

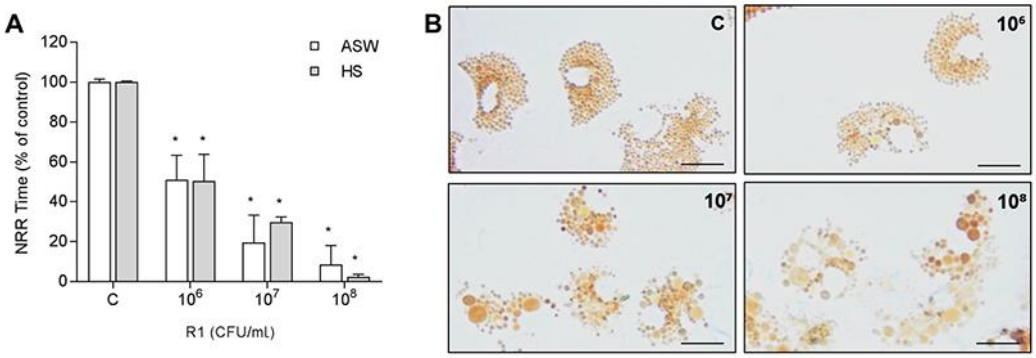

Figure 3. *In vitro* effects of *M. marinus* R1 strain on hemocyte lysosomal membrane stability-LMS.
A) LMS evaluated in different media (ASW or HS). Data, expressed as percent values with respect to controls and representing the mean ± SD of 4 experiments in triplicate. Statistical analyses were performed by non-parametric Kruskal–Wallis followed by Dunn's multiple comparisons test (* = $p < 0.05$).
B) Representative images of control hemocytes (C) and of hemocytes exposed to different concentrations of bacteria (10^6, 10^7, 10^8 CFU/mL in ASW) after loading with NR (time 0). Lysosomes are stained in red, nuclei and intact cytoplasm appear transparent (Scale bar: 10 µm).

Data on functional immune parameters, ROS production and lysozyme release, are reported in Fig. 4. Hemocyte exposure to *M. marinus* R1 suspensions in ASW did not elicit significant extracellular ROS production; however, in the presence of HS, a large increase in ROS was observed at both 10^6 and 10^7 CFU/mL (+350% to +480% respectively, with respect to controls) (Fig. 4A). Lysozyme activity showed small increases (+20-+50% with respect to controls), depending on the time of incubation (30 and 60 min) and exposure medium (Fig. 4B and 4C).

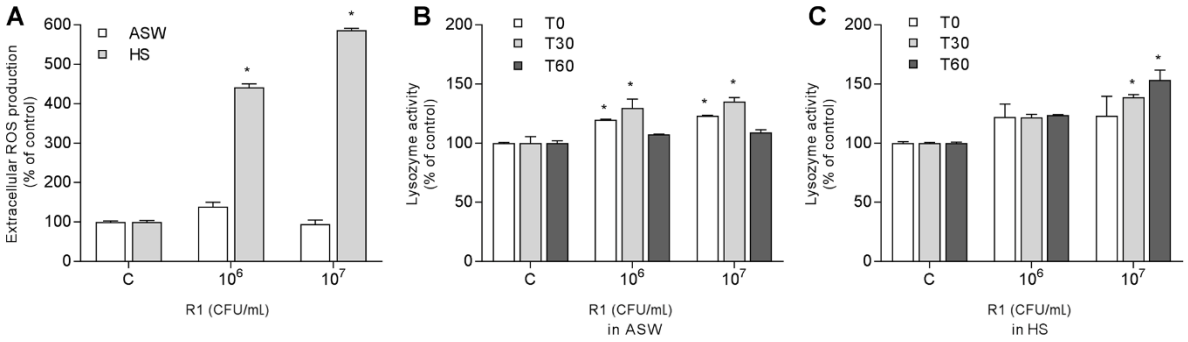

Figure 4. ***In vitro* effects of *M. marinus* R1 on immune responses of *M. galloprovincialis* hemocytes**.
Extracellular ROS production (A) and lysosomal enzyme release (B-C) were evaluated after incubation with R1 at 10^6 and 10^7 CFU/mL in ASW or HS. Hemocytes were incubated for different periods of time (30 min for ROS production and 30 and 60 min for lysozyme release). Data are the mean ± SD of at least 4 experiments performed in triplicate. Statistical analyses were performed by non-parametric Kruskal–Wallis followed by Dunn's multiple comparisons test (* = $p < 0.05$).

Hemocyte monolayers incubated with different concentrations of R1 (10^6 - 10^8 CFU/mL) in ASW for 30 or 90 min, were stained with Giemsa (Fig. 5). At both 30 and 90 min incubation, control hemocytes were well spread on the support, showing different cytoplasmic extensions, with the nuclei colored in dark violet, the cytosol in pink, and intracellular vacuoles and lysosomes (mainly located in the perinuclear region) in pink-yellowish (Fig. 5A and 5 E). After 30 min incubation with R1 (Fig. 5, B-D), an increasing number of bacteria were observed within the hemocytes, on cellular membranes and in the extracellular medium at increasing concentrations. Intracellular bacteria were mainly localized within enlarged lysosomal vesicles,

indicating phagocytosis (black arrowhead). Similar observations were made after 90 min incubation (Fig. 5, F-H), showing still adherent hemocytes with enlarged lysosomes. Moreover, at the highest concentration tested, enlarged vacuoles stained in dark violet were observed at both 30 and 90 min, containing bacteria. Similar results were obtained using bacterial suspensions in HS (not shown).

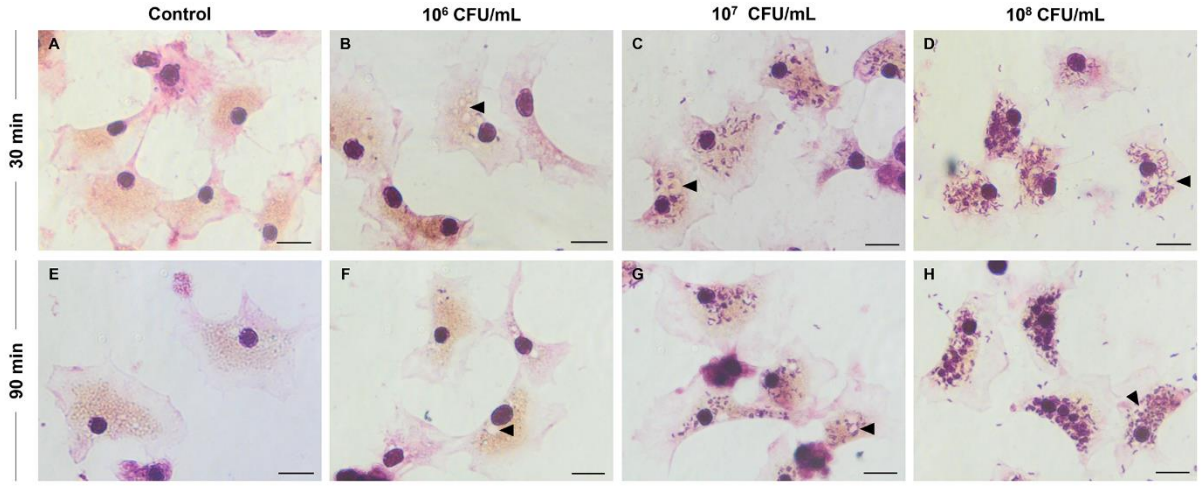

Figure 5. Giemsa staining of control hemocytes and hemocytes incubated with different concentrations of *M. marinus* R1.
Hemocytes were incubated with R1 10^6, 10^7 and 10^8 CFU/mL in ASW for 30 (A-D) and 90 min (E-H). A and E) Controls, B and F) 10^6 CFU/mL, C and G) 10^7 CFU/mL and D and H) 10^8 CFU/mL. Black arrowheads: enlarged lysosomes. Scale bar: 10 µm.

The possible mechanisms involved in *M. marinus* R1-induced lysosomal enlargement and internalization were investigated by evaluating the expression of the autophagic markers LC3 (microtubule-associated protein 1A/1B-light chain 3) and phosphorylated of mTor (mammalian target of rapamycin mTOR) by electrophoresis and Western Blotting [26], and the results are shown in Fig. 6. With regards to LC3, although the antibody can recognize both the LC3-I and LC-II forms, only the band corresponding to the lipidated LC3-II form could be identified in all samples (Fig. 6A). Although we previously identified both bands in mussel hemocytes collected in autumn (October) [26], in the present work, experiments were performed in mussels sampled in early summer. The presence of the LC3-II form only is often observed in different marine invertebrate models ([27] and refs therein); therefore, the differences in results obtained in hemocytes from mussels sampled at different times of the year may reflect seasonal variations in LC expression. The results of the densitometric analysis showed that challenge with R1 induced a large decrease in expression of LC3-II at both 30 and 90 min (about -60% with respect to controls at 30 min). A similar decrease was observed in the level of p-mTor (Fig. 6B). As previously reported [26], no changes in expression of LC3-II or p-mTor were observed in control samples at different times of incubation (not shown).

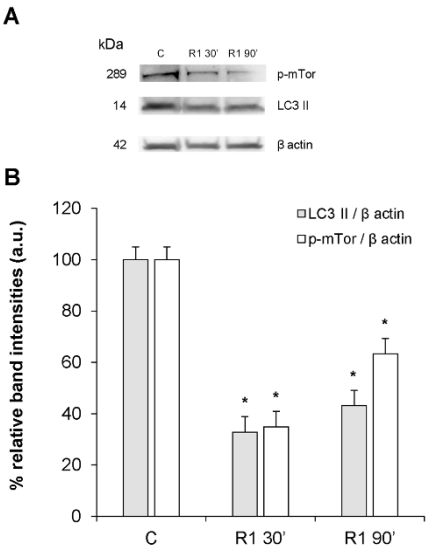

Figure 6. Effects of *M. marinus* R1 on expression levels of LC3 and phosphorylated mTor in *M. galloprovincialis* hemocytes.
Expression of LC3-II and p-mTor in control hemocytes and hemocytes incubated for 30 and 90 min with R1 (10^7 CFU/mL). A) Representative blots, with β actin as a loading control. B) Densitometric analysis of blots from four independent experiments (mean ± SD). * $p \leq 0.05$, Mann-Whitney U test.

Finally, the bactericidal activity of mussel hemocytes towards *M. marinus* R1 (5×10^6 CFU/mL) was evaluated in the presence of ASW or HS, as well as in HS and ASW alone, at 30 and 90 min incubation, and data are expressed as the percentage of killed bacteria with respect time zero (Fig. 7). Hemocytes in ASW showed a significant and time-dependent bactericidal activity (20% and 75%, respectively, at 30 and 90 min). A similar effect was observed using HS alone (30% and 80%). Accordingly, the bactericidal activity was highest in samples of hemocytes in the presence of HS, in particular at shorter times of incubation (60% and 85%, at 30 and 90 min, respectively). No bacterial killing was observed in ASW alone.

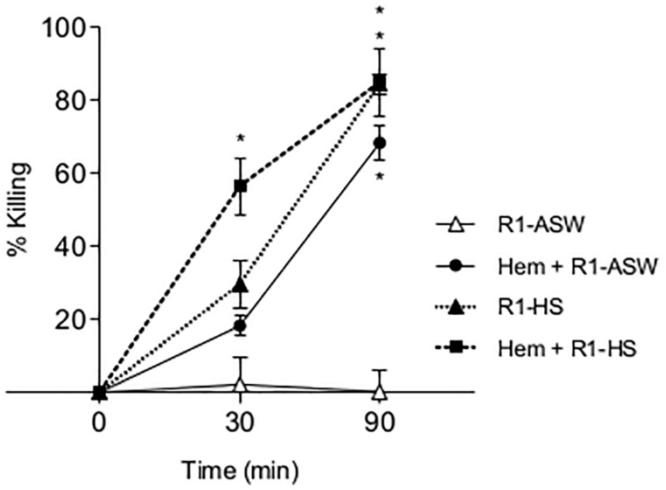

Figure 7. ***In vitro* bactericidal activity of mussel hemocytes and serum towards *M. marinus* R1.**
Hemocytes were incubated for 30 and 90 min with *M. marinus* R1, at 5×10^6 CFU/mL resuspended in either ASW (Hem + R1-ASW) or hemolymph serum (Hem + R1-HS). In parallel, *M. marinus* R1 were incubated in ASW (R1-ASW) or HS (R1-HS) alone. At each time point, the number of viable, cultivable bacteria (CFU) per monolayer was evaluated, and the results are expressed as percentage values with respect to time zero. Statistical analyses

were performed by non-parametric Kruskal–Wallis followed by Dunn's multiple comparisons test, * = $p < 0.05$, all treatments vs control (R1 in ASW).

4. Discussion

The results represent the first data on the interactions of environmental strains of *Arcobacter*-like spp. with marine bivalves. Two strains of *M. marinus* (IRTA-19-131 and IRTA-19-132) isolated from adult diseased oysters collected during a mortality event in the Ebro delta (Spain) were utilized.

Bivalve early developmental stages are likely to be more susceptible to pathogens than adults, since the immune system has not fully developed [28,29]. Therefore, we first tested the effects of *M. marinus* strains R1 and R2 in mussel early larvae utilizing the 48 h embryotoxicity assay. The results show that both strains affected normal larval development in a wide concentration range. Slight differences were observed between the two strains in terms of minimal effective concentrations (with significant effects observed from 10^3 to 10^4 CFU/mL, respectively, for R1 and R2), extent of the effects at the highest concentration tested (with R1 higher than R2), and main phenotypical changes (developmental delay for R1 and larval malformations for R2). Overall, the results indicate that both *M. marinus* strains are moderately pathogenic for early mussel larvae. In the same experimental conditions, stronger effects were observed with different pathogenic vibrios, such as *Vibrio coralliilyticus* [23], *V. tasmaniensis* LGP32, *V. bathopelagicus* sp. nov. [30].

Responses to challenge with *M. marinus* were then investigated in adult mussels *in vivo*, injected with either R1 or R2 (5×10^6 CFU/mL hemolymph) where functional hemolymph parameters were evaluated at 24 h p.i.. The results show that both strains induced similar lysosomal stress in hemocytes (evaluated as a decrease in LMS); however, a large stimulation of extracellular defenses (ROS production and lysozyme activity) was observed, indicating that hemolymph components of adult mussels are able to mount an efficient defense response against *M. marinus* infection.

The mechanisms involved in immune interactions with *M. marinus* were subsequently investigated in *in vitro* short-term experiments in isolated hemocytes exposed for 30 - 90 min in the absence and presence of hemolymph serum (ASW or HS). Since both strains induced a similar concentration dependent effect on hemocyte LMS in a wide concentration range, we chose to utilize only R1 (10^6 - 10^8 CFU/mL) for further investigations. Lysosomal membrane destabilization was similar in the absence and presence of HS, and the effect was accompanied by lysosomal enlargement. However, no hemocyte rounding or detachment, indicating cell death, was observed. R1 induced a large and concentration dependent stimulation of extracellular ROS production in the presence of HS, but not in ASW, indicating a role for soluble components in the recognition of this strain and subsequent activation of membrane NADPH oxidase, the enzyme responsible for ROS production. R1 moderately stimulated the release of lysozyme release in both media, with differences in the extent and time course of the response. The results obtained *in vitro* thus confirm *in vivo* observations, showing that induction of lysosomal stress in the hemocytes was associated with stimulation of extracellular defense mechanisms.

Interactions of *M. marinus* with hemocytes were also investigated in Giemsa stained samples. After 30 min incubation, an increasing number of bacteria were visible inside the hemocytes at increasing concentrations, that were mainly localized within enlarged intracellular vesicles. Although optical microscopy does not allow for the identification of localization of bacteria, the results suggest their phagocytosis and subsequent lysosomal degradation.

With regards to the intracellular mechanisms involved in the response of hemocytes to R1 (lysosomal stress and enlargement, phagocytosis and lysosomal degradation of bacteria in the absence of cytotoxicity), the possible role of autophagic processes was investigated. In mussel hemocytes, we have previously demonstrated a protective role of autophagy against the pathogen *V. tapetis* [26]. *V. tapetis* induced a rapid stimulation of autophagy (induction of autophagosomes, and increase in autophagic markers LC3-II, p-mTor and p62), in the absence of phagocytosis and lysosomal degradation [26].

The results here obtained show that challenge with *M. marinus* resulted in contrasting effects on hemocyte autophagy markers. Although a decrease in mTor phosphorylation, indicating stimulation of autophagy, was observed, a similar effect was also recorded for LC3-II, the activated, lipidated form of LC3, whose increase is considered as an early marker of autophagy. Moreover, no changes in expression of p62 were observed (not shown). Overall, the results do not support an induction of the autophagic flux in mussel hemocytes by this strain of *M. marinus*. However, these data could be explained when considering by the multiple roles of mTor and LC3 in immune response. mTOR is a master kinase that also regulates lysosome structure and function and innate immunity; in macrophages, *V. vulnificus* induces mTor activation and inflammatory responses [31]. LC3 is also involved in LAP (LC3-associated phagocytosis), a form of non-canonical autophagy, best characterized in the clearance of pathogens by macrophages [32]. Briefly, in LAP, LC3 is conjugated to phagosome membranes while the bacterium is captured in the phagosome, thus acting as an innate immune response mechanism [32,33]. Unlike autophagy, LAP involves single-membrane structures, and a distinct rate of activation of LC3. Accordingly, in macrophages stimulated with *Candida albicans*, activated LC3 was increased at the peak of phagocytosis, and decreased at later times, when the process was completed [34]. In the present work, a similar condition is observed in mussel hemocytes during phagocytosis of *M. marinus* R1, indicating a decrease in LC3-II at 30-90 min, when the phagocytic process is well advanced or completed. These data provide the first indication for LAP, a unique process that links the ancient pathways of phagocytosis and autophagy in invertebrate immunocytes [35].

Finally, the bactericidal activity of hemolymph components was quantified by evaluating the percentage of killed bacteria in different experimental conditions, utilizing a concentration of R1 (5×10^6 CFU/mL) that induced both lysosomal stress and induction of extracellular defenses. After 30 min, a small bactericidal activity was shown by both hemocytes and HS alone (20% and 30% respectively). This activity could be ascribed to the extracellular release of ROS and enzymatic defenses (lysozyme) from hemocytes (Fig. 4) and to the direct effects of soluble serum components. A cumulative effect was observed for hemocytes in the presence of HS. Hemocytes alone showed a stronger bactericidal activity at longer incubation times (90 min), (up to 75%) this increase probably reflects the time needed for recognition of R1 in absence of HS, and consequent phagocytosis and lysosomal degradation. Maximal killing activity was observed with hemocytes in the presence of HS (85%). Although the components of HS involved in mediating immune defenses towards *M. marinus* strains were not identified, the results support the hypothesis that *Mytilus* hemolymph contains specific soluble factors that contribute to the general killing of many bacteria that are strongly pathogenic for other bivalve species [36,37].

The results obtained in *in vitro* experiments on the interactions between *M. marinus* strains and mussel hemocytes can be compared with previous data with other potentially pathogenic marine bacteria from the genus *Vibrio* tested in the same experimental conditions (Table 1). Among the most pathogenic vibrios for bivalves, *V. coralliilyticus* ATCC BAA-450 and *V. tasmaniensis* LGP32 induced strong cellular stress in the absence of efficient immune response and bactericidal activity [23,25]. Responses to *V. tapetis* consisted in absence or inhibition of immune responses [26]. *V. aestuarianus* 01/032 induced moderate stress in hemocytes where it

was rapidly internalized and degraded by phagocytosis [25]. Environmental isolates of *V. parahaemolyticus* and *V. alginolyticus* elicited efficient immune responses, whereas *V. vulnificus* induced slower and minor responses with apoptosis [38]. The results obtained so far demonstrate that mussel hemocytes show different susceptibilities to different potential pathogens, according to the species and strain, reflecting specificities in pathogen recognition, binding and consequent activation of extracellular and intracellular defenses. Although the mechanisms involved in these specific interactions can be easily identified *in vitro*, the observed outcome of the response is generally observed also *in vivo* ([25], this work).

	LMS	**ROS**	**Lyso. act**	**Killing**
M. marinus R1	↓↓↓	↑↑↑	↑	↑↑↑
V. coralliilyticus[1]	↓↓↓	≈	nd	≈
V. tasmaniensis[2]	↓↓↓	nd	↑↑	≈
V. aestuarianus[2]	≈	nd	↑	↑
V. tapetis[3]	↓	↓↓	≈	≈
V. parahaemolyticus[4]	↓↓	↑	↑	nd

Table 1. Summary of *in vitro* data on immune parameters in *M. galloprovincialis* hemocytes challenged with *M. marinus* R1 and different *Vibrio* (10^7 CFU/mL) in the presence of HS. The parameters reported include: lysosomal membrane stability (LMS), extracellular ROS production and lysozyme release, expressed as % of control values. Bactericidal activity is reported as % of killed bacteria with respect to the inoculum.
[1]*V. coralliilyticus* ATCC BAA-450 [23], [2]*V. tasmaniensis* LGP32 and *V. aestuarianus* 01/032 [25], [3]*V. tapetis* LP2 [26]. [4]*V. parahaemolyticus* Conero 80 [38]. nd: not determined. ↓: decreased; ↑: increase; ≈ no effect.

On the basis of the overall data, the *M. marinus* strain R1 utilized in the present work is among the less pathogenic to mussels under laboratory conditions. However, the increased *in vivo* abundance of members of the *Arcobacter*-like spp. in stressed or diseased bivalve species, often in association with more pathogenic *Vibrio* [4], indicates that the interactions with the immune system of the host are extremely sensitive to perturbations by environmental factors or concomitant infections with pathogens, resulting in a strongly opportunistic behavior of *Arcobacter*. In this light, the role of the non-virulent microbiota should not be neglected, as non-virulent *Vibrio* strains have the potential to dramatically increase the host damages caused by virulent strains [4]. Data from co-challenge experiments with pathogenic and opportunistic bacteria may help understanding these interactions. Moreover, edible bivalves can vehiculate *Arcobacter*-like species up to humans, as shown by a recently reported case of human bacteremia induced by *M. mytili* [39]. Further information is also needed on the interactions of *Arcobacter* strains with the immune system of other bivalves; in particular research is in progress on the interactions between *M. marinus* strains and immune system of the oyster *C. gigas*.

Supplementary Materials

Figure S1: Effects of different concentrations of two *M. marinus* strains R1 and R2 on hemocyte lysosomal membrane stability (LMS).
Figure S2. Representative images of hemocytes exposed to *M. marinus* strains R1 at the end of the NRR assay (120 min).

Funding

This work was supported by the Italian Ministry of University and Research (MUR), PRIN 2017 code: 201728ZA49_002. T.B. was supported by a grant Fondi Ricerca Ateneo (FRA)

from Università di Genova, (100022-2020-FRA2019-Balbi). M.L. was supported by a Starting grant from Università di Genova.

Declaration of interest

Declarations of interest: none

CRediT authorship contribution statement

Manon Auguste: Conceptualization; Data curation; Formal analysis; Investigation; Roles/Writing - original draft; Writing - review & editing.
Faiz Ur Rahman : Methodology; Formal analysis
Teresa Balbi : Conceptualization; Data curation; Software
Martina Leonessi : Data curation; Formal analysis; Investigation
Caterina Oliveri : Data curation; Formal analysis; Investigation
Grazia Bellese : Formal analysis
Luigi Vezzulli : Conceptualization; Resources; Supervision; Writing - review & editing.
Dolors Furones : Resources; Supervision; Writing - review & editing.
Laura Canesi : Conceptualization; Supervision; Roles/Writing - original draft; Writing - review & editing.

References

[1] M. Charles, I. Bernard, A. Villalba, E. Oden, E.A.V. Burioli, G. Allain, S. Trancart, V. Bouchart, M. Houssin, High mortality of mussels in northern Brittany – Evaluation of the involvement of pathogens, pathological conditions and pollutants, J. Invertebr. Pathol. 170 (2020) 107308. https://doi.org/10.1016/j.jip.2019.107308.

[2] L. Avdelas, E. Avdic-Mravlje, A.C. Borges Marques, S. Cano, J.J. Capelle, N. Carvalho, M. Cozzolino, J. Dennis, T. Ellis, J.M. Fernández Polanco, J. Guillen, T. Lasner, V. Le Bihan, I. Llorente, A. Mol, S. Nicheva, R. Nielsen, H. Oostenbrugge, S. Villasante, S. Visnic, K. Zhelev, F. Asche, The decline of mussel aquaculture in the European Union: causes, economic impacts and opportunities, Rev. Aquac. 13 (2021) 91–118. https://doi.org/10.1111/raq.12465.

[3] B. Petton, D. Destoumieux-Garzón, F. Pernet, E. Toulza, J. de Lorgeril, L. Degremont, G. Mitta, The Pacific Oyster Mortality Syndrome, a Polymicrobial and Multifactorial Disease: State of Knowledge and Future Directions, Front. Immunol. 12 (2021) 630343. https://doi.org/10.3389/fimmu.2021.630343.

[4] D. Destoumieux-Garzón, L. Canesi, D. Oyanedel, M. Travers, G.M. Charrière, C. Pruzzo, L. Vezzulli, *Vibrio* –bivalve interactions in health and disease, Environ. Microbiol. 22 (2020) 4323–4341. https://doi.org/10.1111/1462-2920.15055.

[5] A. Lasa, A. di Cesare, G. Tassistro, A. Borello, S. Gualdi, D. Furones, N. Carrasco, D. Cheslett, A. Brechon, C. Paillard, A. Bidault, F. Pernet, L. Canesi, P. Edomi, A. Pallavicini, C. Pruzzo, L. Vezzulli, Dynamics of the Pacific oyster pathobiota during mortality episodes in Europe assessed by 16S rRNA gene profiling and a new target enrichment next-generation sequencing strategy, Environ. Microbiol. 21 (2019) 4548–4562. https://doi.org/10.1111/1462-2920.14750.

[6] M. Richard, J.L. Rolland, Y. Gueguen, J. de Lorgeril, J. Pouzadoux, B. Mostajir, B. Bec, S. Mas, D. Parin, P. Le Gall, S. Mortreux, A. Fiandrino, F. Lagarde, G. Messiaen, M. Fortune, E. Roque d'Orbcastel, In situ characterisation of pathogen dynamics during a Pacific oyster mortality syndrome episode, Mar. Environ. Res. 165 (2021) 105251. https://doi.org/10.1016/j.marenvres.2020.105251.

[7] J. de Lorgeril, A. Lucasson, B. Petton, E. Toulza, C. Montagnani, C. Clerissi, J. Vidal-Dupiol, C. Chaparro, R. Galinier, J.-M. Escoubas, P. Haffner, L. Dégremont, G.M. Charrière, M. Lafont, A. Delort, A. Vergnes, M. Chiarello, N. Faury, T. Rubio, M.A. Leroy, A. Pérignon, D. Régler, B. Morga, M. Alunno-Bruscia, P. Boudry, F. Le Roux, D. Destoumieux-Garzón, Y. Gueguen, G. Mitta, Immune-suppression by OsHV-1 viral infection causes fatal bacteraemia in Pacific oysters, Nat. Commun. 9 (2018). https://doi.org/10.1038/s41467-018-06659-3.

[8] A. Lokmer, K. Mathias Wegner, Hemolymph microbiome of Pacific oysters in response to temperature, temperature stress and infection, ISME J. 9 (2015) 670–682. https://doi.org/10.1038/ismej.2014.160.

[9] Y.-F. Li, N. Yang, X. Liang, A. Yoshida, K. Osatomi, D. Power, F.M. Batista, J.-L. Yang, Elevated Seawater Temperatures Decrease Microbial Diversity in the Gut of Mytilus coruscus, Front. Physiol. 9 (2018). https://doi.org/10.3389/fphys.2018.00839.

[10] M. Auguste, A. Lasa, T. Balbi, A. Pallavicini, L. Vezzulli, L. Canesi, Impact of nanoplastics on hemolymph immune parameters and microbiota composition in Mytilus galloprovincialis, Mar. Environ. Res. 159 (2020) 105017. https://doi.org/10.1016/j.marenvres.2020.105017.

[11] C.D. Iwu, T.C. Ekundayo, A.I. Okoh, A Systematic Analysis of Research on Arcobacter: Public Health Implications from a Food–Environment Interphase Perspective, Foods. 10 (2021) 1673. https://doi.org/10.3390/foods10071673.

[12] J.C. Fisher, A. Levican, M.J. Figueras, S.L. McLellan, Population dynamics and ecology of Arcobacter in sewage, Front. Microbiol. 5 (2014). https://doi.org/10.3389/fmicb.2014.00525.

[13] J. Romero, M. García-Varela, J.P. Laclette, R.T. Espejo, Bacterial 16S rRNA Gene Analysis Revealed That Bacteria Related to Arcobacter spp. Constitute an Abundant and Common Component of the Oyster Microbiota (Tiostrea chilensis), Microb. Ecol. 44 (2002) 365–371. https://doi.org/10.1007/s00248-002-1063-7.

[14] F. Fanelli, A. Di Pinto, A. Mottola, G. Mule, D. Chieffi, F. Baruzzi, G. Tantillo, V. Fusco, Genomic Characterization of Arcobacter butzleri Isolated From Shellfish: Novel Insight Into Antibiotic Resistance and Virulence Determinants, Front. Microbiol. 10 (2019) 670. https://doi.org/10.3389/fmicb.2019.00670.

[15] L. Collado, I. Cleenwerck, S. Van Trappen, P. De Vos, M.J. Figueras, Arcobacter mytili sp. nov., an indoxyl acetate-hydrolysis-negative bacterium isolated from mussels, Int. J. Syst. Evol. Microbiol. 59 (2009) 1391–1396. https://doi.org/10.1099/ijs.0.003749-0.

[16] F. Leoni, S. Chierichetti, S. Santarelli, G. Talevi, L. Masini, C. Bartolini, E. Rocchegiani, M. Naceur Haouet, D. Ottaviani, Occurrence of Arcobacter spp. and correlation with the bacterial indicator of faecal contamination Escherichia coli in bivalve molluscs from the Central Adriatic, Italy, Int. J. Food Microbiol. 245 (2017) 6–12. https://doi.org/10.1016/j.ijfoodmicro.2017.01.006.

[17] A. Mottola, E. Bonerba, M.J. Figueras, A. Pérez-Cataluña, P. Marchetti, A. Serraino, G. Bozzo, V. Terio, G. Tantillo, A. Di Pinto, Occurrence of potentially pathogenic arcobacters in shellfish, Food Microbiol. 57 (2016) 23–27. https://doi.org/10.1016/j.fm.2015.12.010.

[18] A.G. Mudadu, S. Salza, R. Melillo, L. Mara, G. Piras, C. Spanu, G. Terrosu, A. Fadda, S. Virgilio, T. Tedde, Prevalence and pathogenic potential of Arcobacter spp. isolated from edible bivalve molluscs in Sardinia, Food Control. 127 (2021) 108139. https://doi.org/10.1016/j.foodcont.2021.108139.

[19] F.U. Rahman, K.B. Andree, N. Salas-Massó, M. Fernandez-Tejedor, A. Sanjuan, M.J. Figueras, M.D. Furones, Improved culture enrichment broth for isolation of Arcobacter-like species from the marine environment, Sci. Rep. 10 (2020) 14547. https://doi.org/10.1038/s41598-020-71442-8.

[20] N. Salas-Massó, Q.T. Linh, W.H. Chin, A. Wolff, K.B. Andree, M.D. Furones, M.J. Figueras, D.D. Bang, The Use of a DNA-Intercalating Dye for Quantitative Detection of Viable Arcobacter spp. Cells (v-qPCR) in Shellfish, Front. Microbiol. 10 (2019) 368. https://doi.org/10.3389/fmicb.2019.00368.

[21] N. Salas-Massó, K.B. Andree, M.D. Furones, M.J. Figueras, Enhanced recovery of Arcobacter spp. using NaCl in culture media and re-assessment of the traits of Arcobacter marinus and Arcobacter halophilus isolated from marine water and shellfish, Sci. Total Environ. 566–567 (2016) 1355–1361. https://doi.org/10.1016/j.scitotenv.2016.05.197.

[22] R. Fabbri, M. Montagna, T. Balbi, E. Raffo, F. Palumbo, L. Canesi, Adaptation of the bivalve embryotoxicity assay for the high throughput screening of emerging contaminants in Mytilus galloprovincialis, Mar. Environ. Res. 99 (2014) 1–8. https://doi.org/10.1016/j.marenvres.2014.05.007.

[23] T. Balbi, M. Auguste, K. Cortese, M. Montagna, A. Borello, C. Pruzzo, L. Vezzulli, L. Canesi, Responses of Mytilus galloprovincialis to challenge with the emerging marine

pathogen Vibrio coralliilyticus, Fish Shellfish Immunol. 84 (2019) 352–360. https://doi.org/10.1016/j.fsi.2018.10.011.

[24] ASTM E724-21, Standard Guide for Conducting Static Short-Term Chronic Toxicity Tests Starting with Embryos of Four Species of Saltwater Bivalve Molluscs, (2021). https://doi.org/10.1520/E0724-21.

[25] T. Balbi, R. Fabbri, K. Cortese, A. Smerilli, C. Ciacci, C. Grande, L. Vezzulli, C. Pruzzo, L. Canesi, Interactions between Mytilus galloprovincialis hemocytes and the bivalve pathogens Vibrio aestuarianus 01/032 and Vibrio splendidus LGP32, Fish Shellfish Immunol. 35 (2013) 1906–1915. https://doi.org/10.1016/j.fsi.2013.09.027.

[26] T. Balbi, K. Cortese, C. Ciacci, G. Bellese, L. Vezzulli, C. Pruzzo, L. Canesi, Autophagic processes in Mytilus galloprovincialis hemocytes: Effects of Vibrio tapetis, Fish Shellfish Immunol. 73 (2018) 66–74. https://doi.org/10.1016/j.fsi.2017.12.003.

[27] R. Chiarelli, M. Agnello, M.C. Roccheri, Sea urchin embryos as a model system for studying autophagy induced by cadmium stress, Autophagy. 7 (2011) 1028–1034. https://doi.org/10.4161/auto.7.9.16450.

[28] P. Balseiro, R. Moreira, R. Chamorro, A. Figueras, B. Novoa, Immune responses during the larval stages of Mytilus galloprovincialis: Metamorphosis alters immunocompetence, body shape and behavior, Fish Shellfish Immunol. 35 (2013) 438–447. https://doi.org/10.1016/j.fsi.2013.04.044.

[29] X. Song, H. Wang, L. Xin, J. Xu, Z. Jia, L. Wang, L. Song, The immunological capacity in the larvae of Pacific oyster Crassostrea gigas, Fish Shellfish Immunol. 49 (2016) 461–469. https://doi.org/10.1016/j.fsi.2016.01.009.

[30] A. Lasa, M. Auguste, A. Lema, C. Oliveri, A. Borello, E. Taviani, G. Bonello, L. Doni, A.D. Millard, M. Bruto, J.L. Romalde, M. Yakimov, T. Balbi, C. Pruzzo, L. Canesi, L. Vezzulli, A deep-sea bacterium related to coastal marine pathogens, Environ. Microbiol. 23 (2021) 5349–5363. https://doi.org/10.1111/1462-2920.15629.

[31] D.-L. Xie, M.-M. Zheng, Y. Zheng, H. Gao, J. Zhang, T. Zhang, J.-C. Guo, X.F. Yang, X.-P. Zhong, Y.-L. Lou, Vibrio vulnificus induces mTOR activation and inflammatory responses in macrophages, PLOS ONE. 12 (2017) e0181454. https://doi.org/10.1371/journal.pone.0181454.

[32] B.L. Heckmann, E. Boada-Romero, L.D. Cunha, J. Magne, D.R. Green, LC3-Associated Phagocytosis and Inflammation, J. Mol. Biol. 429 (2017) 3561–3576. https://doi.org/10.1016/j.jmb.2017.08.012.

[33] B.L. Heckmann, D.R. Green, LC3-associated phagocytosis at a glance, J. Cell Sci. 132 (2019) jcs222984. https://doi.org/10.1242/jcs.222984.

[34] Z. Duan, Q. Chen, L. Du, J. Tong, S. Xu, R. Zeng, Y. Ma, X. Chen, M. Li, Phagocytosis of *Candida albicans* Inhibits Autophagic Flux in Macrophages, Oxid. Med. Cell. Longev. 2018 (2018) 1–14. https://doi.org/10.1155/2018/4938649.

[35] D. Klionsky, A.K. Abdel-Aziz, S. Abdelfatah, M. Abdellatif, et al., Guidelines for the use and interpretation of assays for monitoring autophagy (4th edition), Autophagy. 17:1 (2021) 1–382. https://doi.org/10.1080/15548627.2020.1797280.

[36] E. Pezzati, L. Canesi, G. Damonte, A. Salis, F. Marsano, C. Grande, L. Vezzulli, C. Pruzzo, Susceptibility of *V ibrio aestuarianu* s 01/032 to the antibacterial activity of *M ytilus* haemolymph: identification of a serum opsonin involved in mannose-sensitive interactions: *Vibrio aestuarianus* and bivalve haemocytes, Environ. Microbiol. 17 (2015) 4271–4279. https://doi.org/10.1111/1462-2920.12750.

[37] L. Canesi, C. Grande, E. Pezzati, T. Balbi, L. Vezzulli, C. Pruzzo, Killing of Vibrio cholerae and Escherichia coli Strains Carrying D-mannose-sensitive Ligands by Mytilus Hemocytes is Promoted by a Multifunctional Hemolymph Serum Protein, Microb. Ecol. 72 (2016) 759–762. https://doi.org/10.1007/s00248-016-0757-1.

[38] C. Ciacci, A. Manti, B. Canonico, R. Campana, G. Camisassi, W. Baffone, L. Canesi, Responses of Mytilus galloprovincialis hemocytes to environmental strains of Vibrio parahaemolyticus, Vibrio alginolyticus, Vibrio vulnificus, Fish Shellfish Immunol. 65 (2017) 80–87. https://doi.org/10.1016/j.fsi.2017.04.002.

[39] M. Vasiljevic, A.J. Fenwick, S. Nematollahi, V.P. Gundareddy, M. Romagnoli, J. Zenilman, K.C. Carroll, First Case Report of Human Bacteremia With Malacobacter (Arcobacter) mytili, Open Forum Infect. Dis. 6 (2019) ofz319. https://doi.org/10.1093/ofid/ofz319.

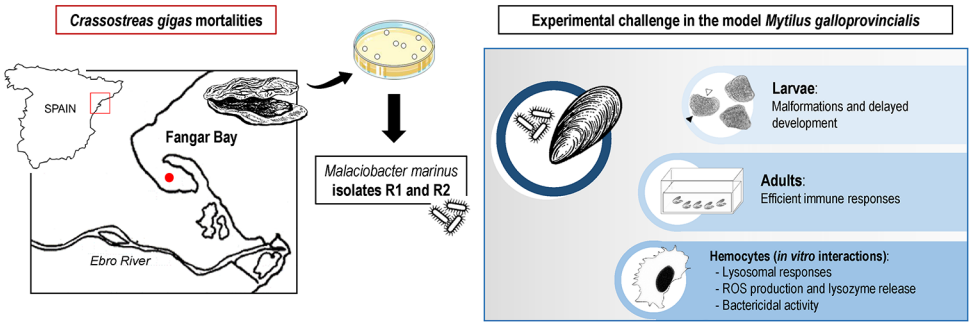
Crassostreas gigas mortalities
SPAIN
Fangar Bay
Ebro River
Malaciobacter marinus
isolates R1 and R2
Experimental challenge in the model *Mytilus galloprovincialis*
Larvae:
Malformations and delayed development
Adults:
Efficient immune responses
Hemocytes (*in vitro* interactions):
- Lysosomal responses
- ROS production and lysozyme release
- Bactericidal activity